Journal of Fluids and Structures (1998) **12,** 367–385

VIBRATION OF A HYDROELASTIC SYSTEM CONSISTING OF A SECTOR SHELL AND VISCOUS LIQUID IN ZERO GRAVITY

H. F. Bauer

Institute für Raumfahrttechnik, Universität der Bundeswehr München
85579 Neubiberg, Germany

AND

K. Komatsu
Structural Mechanics Division, National Aerospace Laboratory, Chofu, Tokyo 182, Japan

(Received 27 June 1997 and in revised form 12 September 1997)

For a circular sector system consisting of an elastic shell to which an incompressible and viscous liquid layer is attached, the coupled liquid-structure frequencies are determined under zero gravity conditions. The influence of the viscosity of the liquid, the flexibility of the shell, the thickness of the liquid layer and the Ohnesorge number have been determined for freely slipping and anchored contact lines. With increasing shell flexibility the oscillation frequencies decrease and exhibit a smaller magnitude for a viscous liquid than for a frictionless liquid. In addition, we observe a phenomenon not present in a system with frictionless liquid, involving regions of only aperiodic motion. In these regions, depending mainly on viscosity (Ohnesorge number) and liquid layer thickness, the hydroelastic system cannot perform any oscillatory motion. A motion identification chart is presented showing that for large Ohnesorge number $\mathrm{Oh} \equiv (\rho v^2/\sigma a)^{1/2}$ only very thick liquid layers are able to perform oscillatory motions. Increasing the flexibility of the shell results in an increased region of aperiodic motion.

1. INTRODUCTION

The era of the international space station where systems are exposed to longer periods of a zero or microgravity environment presents us with unique manufacturing and chemical engineering processing possibilities, which by no means would be possible on earth under normal gravity conditions. Cylindrical configurations seem to be the basic geometry that will be employed in the structure of the system as well as in space experiments. Since the structures should be light, they will by necessity be highly flexible. Moreover, they will interact with liquids with a free surface.

Various investigations have been performed previously on rotating and nonrotating liquids contained in rigid structures under normal or increased gravity conditions (Abramson 1966) and in a zero gravity environment (Bauer 1982). Investigations with no axial (z)-dependency may be found in Bauer (1987*a*). In a cylindrical configuration, the liquid column exhibits Rayleigh instability in the axisymmetric mode, becoming unstable if the length equals or exceeds the length of the circumference of the column (Rayleigh 1882). This

0889–9746/98/030367 + 19 $25.00/fl970138

is valid for frictionless, viscous, and even viscoelastic liquids (Bauer 1986, 1989). The hydroelastic system, where the sloshing liquid interacts with the flexible structure has also been treated for cylindrical structural systems with a liquid layer on the inside or outside of the elastic cylindrical shell. Results of coupled liquid and coupled shell frequencies were obtained for both a frictionless liquid (Bauer 1987*b*) and a viscous liquid (Bauer 1987*c*). While in a z-independent circular cylindrical system no instability occurs, in a sector system instability appears for certain apex angles (sector openings).

In addition, in many engineering areas, hydroelastic problems have become of increasing interest; in most cases, the structures are thin, they are of high flexibility, and they react with liquids with a free surface of close natural frequencies. In most investigations, however, experimental and theoretical analysis has been centred on upright circular cylindrical containers [e.g., Yamaki *et al.* (1984), Lakis & Païdoussis (1971), and many more].

Recently, the interaction of a sector-shell structure with a liquid layer consisting of incompressible and frictionless liquid and placed in a zero gravity environment has been treated (Bauer & Komatsu 1994). Two main cases for the contact lines at the straight rigid sector walls, i.e., freely slipping and anchored edges were considered. It was found that the natural liquid frequencies with anchored contact lines are larger than those with freely slipping edges, and that thinner liquid layers exhibit decreased natural frequencies. In addition, the uncoupled clamped shell frequencies decrease rapidly with increasing shell radius. The coupled liquid and structural frequencies are lower, an effect that becomes more pronounced for thin liquid layers. It was also found that the interaction effects are stronger if the contact lines are anchored.

The aim of the present investigation is to find the influence of viscosity of the liquid upon the coupled frequencies and to obtain more information on the effect of liquid layer thickness, flexibility, and the Ohnesorge number, which is a measure of the combined effect of liquid surface tension and viscosity. The side walls (radial walls) are considered rigid, while the description of the shell motion is achieved by employing the Donnell shell equation (Leissa 1973). The liquid layer is considered incompressible and viscous, exhibits a liquid surface tension, and is considered either free to slip or develops anchored contact lines at the side walls.

2. BASIC EQUATIONS

A viscous liquid in contact with an elastic structure performs hydroelastic damped vibrations, if disturbed. The problem to be treated here is the determination of the coupled frequencies of a viscous liquid of volume $V_0 = \pi\alpha(a^2 - b^2)$ inside or outside an elastic sector shell. For small elastic displacements of the shell, ξ and η, and small velocity components of the liquid, u and v, the governing equations may be linearized.

The motion of the liquid surrounding a sector shell (Figure 1) is obtained by solving the Stokes equations:

$$\frac{1}{\nu}\frac{\partial u}{\partial t} + \frac{1}{\mu}\frac{\partial p}{\partial r} = \frac{\partial^2 u}{\partial r^2} + \frac{1}{r}\frac{\partial u}{\partial r} - \frac{u}{r^2} + \frac{1}{r^2}\frac{\partial^2 u}{\partial \varphi^2} - \frac{2}{r^2}\frac{\partial v}{\partial \varphi}, \tag{1}$$

$$\frac{1}{\nu}\frac{\partial v}{\partial t} + \frac{1}{\mu}\frac{\partial p}{\partial \varphi} = \frac{\partial^2 v}{\partial r^2} + \frac{1}{r}\frac{\partial v}{\partial r} - \frac{v}{r^2} + \frac{1}{r^2}\frac{\partial^2 v}{\partial \varphi^2} - \frac{2}{r^2}\frac{\partial v}{\partial \varphi}, \tag{2}$$

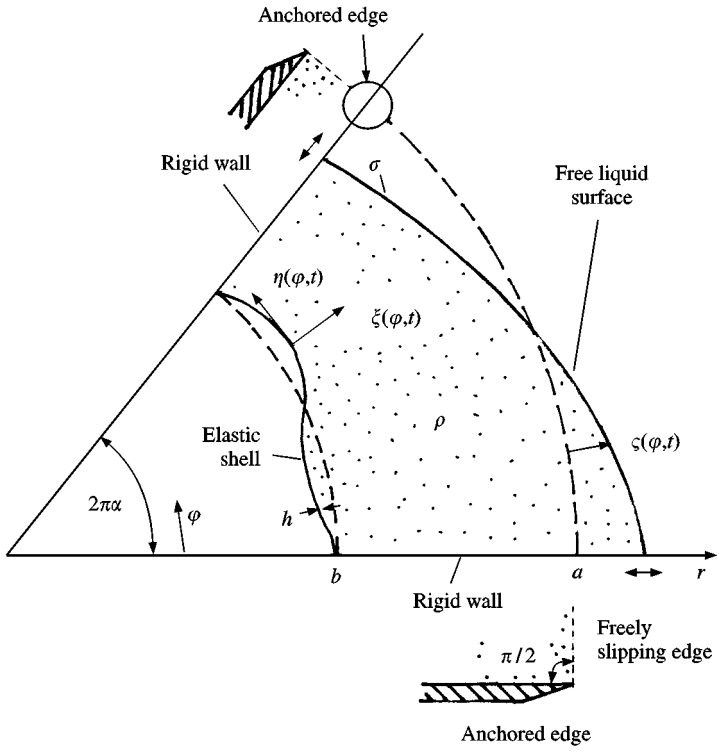

Figure 1. Geometry of the hydroelastic system.

and the continuity equation

$$\frac{\partial u}{\partial r} + \frac{u}{r} + \frac{1}{r}\frac{\partial v}{\partial \varphi} = 0. \tag{3}$$

In these equations, μ is the dynamic viscosity and $\nu = \mu/\rho$ the kinematic viscosity of the incompressible liquid of density ρ. The flow velocity is given by $\mathbf{v} = u\mathbf{e}_r + v\mathbf{e}_\varphi$, and p represents the pressure distribution.

These equations have to be solved with the appropriate boundary conditions. At the rigid side walls vanishing velocity, the following conditions must be satisfied:

$$u = 0,\ v = 0 \qquad \text{at } \varphi = 0 \text{ and } 2\pi\alpha; \tag{4}$$

while at the free liquid surface, the kinematic condition

$$\frac{\partial \zeta}{\partial t} = u \qquad \text{at } r = a, \tag{5}$$

and the dynamic condition

$$\frac{\partial^2 \zeta}{\partial \varphi^2} + \zeta = -\frac{pa^2}{\sigma} + \frac{2\mu a^2}{\sigma}\frac{\partial u}{\partial r} \qquad \text{at } r = a, \tag{6}$$

should be satisfied, where $\zeta = \zeta(\varphi, t)$ is the free liquid surface displacement and σ the liquid surface tension. In addition, the shear stress at the free liquid surface must vanish, i.e.,

$$\tau_{r\varphi} = \mu\left[r\frac{\partial}{\partial r}\left(\frac{v}{r}\right) + \frac{1}{r}\frac{\partial u}{\partial \varphi}\right] = 0 \qquad \text{at } r = a. \tag{7}$$

If we denote the elastic deflection of the shell by $\xi(\varphi, t)$ in the radial direction and $\eta(\varphi, t)$ in the circumferential direction, the equations of the cylindrical shell of infinite length may (under the assumption of no motion in z-direction) be written (Leissa 1973) as

$$\frac{\partial^4 \xi}{\partial \varphi^4} + 2\frac{\partial^2 \xi}{\partial \varphi^2} + \left[1 + \frac{12b^2}{h^2}\right]\xi + \frac{12b^2}{h^2}\frac{\partial \eta}{\partial \varphi} + \frac{12\bar{\rho}(1-\bar{\nu}^2)b^4}{Eh^2}\frac{\partial^2 \xi}{\partial t^2} = -\frac{12b^4}{\bar{D}h^2}\left[p - 2\mu\frac{\partial u}{\partial r}\right]_{r=b} \tag{8}$$

and

$$\frac{\partial \xi}{\partial \varphi} + \frac{\partial^2 \eta}{\partial \varphi^2} - \frac{\bar{\rho}(1-\bar{\nu}^2)b^2}{E}\frac{\partial^2 \eta}{\partial t^2} = \frac{b^2\mu}{\bar{D}}\left[r\frac{\partial}{\partial r}\left(\frac{v}{r}\right) + \frac{1}{r}\frac{\partial u}{\partial \varphi}\right]_{r=b}, \tag{9}$$

where $\bar{\rho}$ is the mass density of the shell, $\bar{\nu}$ is the Poisson ratio, E the elasticity modulus, h the thickness of the shell, and $\bar{D} = Eh/(1-\bar{\nu}^2)$. As we may notice, these equations are coupled with the liquid motion on the right-hand side by pressure and shear forces. We have employed a form of Donnell's shell equations, which are widely used in shallow shell theory. They could easily be extended into Flügge's shell equations by supplying additional terms in the r-direction.

3. METHOD OF SOLUTION

Since the foregoing set of equations cannot be solved exactly by analytical means, we shall treat two cases approximately. In the first case, we abandon the boundary condition $u = 0$ at $\varphi = 0$ and $2\pi\alpha$, and let the liquid slip at the rigid walls; all other conditions will be satisfied. The second case abandons the same condition but enforces the condition that the free liquid surface be anchored at $\varphi = 0$ and $2\pi\alpha$. The first case is called *the freely slipping edge case*; while the second case is called *the anchored-edge condition*, $\zeta(0, t) = \zeta(2\pi\alpha, t) = 0$. In addition, we shall investigate the uncoupled liquid and shell cases.

3.1. Uncoupled Viscous Liquid Motion with Freely Slipping Edges

If the shell wall $r = b$ is considered rigid, we deal only with the oscillation of a viscous liquid. Consequently, equations (1)–(7) have to be solved simultaneously. For the case of freely slipping edges we omit $u = 0$ at $\varphi = 0$ and $2\pi\alpha$. Introducing the stream function $\Psi(\varphi, t)$, such that the continuity equation (3) is identically satisfied, i.e.,

$$u = -\frac{1}{r}\frac{\partial \Psi}{\partial \varphi}, \qquad v = \frac{\partial \Psi}{\partial r}, \tag{10}$$

we obtain, after eliminating the pressure from the Stokes equations (1) and (2), the partial differential equation

$$\nabla^2\left[\nabla^2\Psi - \frac{1}{v}\frac{\partial\Psi}{\partial t}\right] = 0, \tag{11}$$

with

$$\nabla^2 \equiv \frac{\partial^2}{\partial r^2} + \frac{1}{r}\frac{\partial}{\partial r} + \frac{1}{r^2}\frac{\partial^2}{\partial\varphi^2}.$$

Applying the divergence operator to the Stokes equations yields the Laplace equation for the pressure

$$\nabla^2 p = 0 \tag{12}$$

Next, considering the functional form

$$\Psi(r, \varphi, t) = \sum_{m=1}^{\infty} \Psi_m^*(r) \sin\left(\frac{m}{2\alpha}\varphi\right) e^{st}, \tag{13}$$

where s is the complex frequency, equation (11) yields

$$\nabla^{*2}\left[\nabla^{*2}\Psi_m^* - \frac{s}{v}\Psi_m^*\right] = 0, \tag{14}$$

where the operator

$$\nabla^{*2} \equiv \frac{d^2}{dr^2} + \frac{1}{r}\frac{d}{dr} - \frac{m^2}{4\alpha^2 r^2}.$$

The solution of equation (11) is given by

$$\Psi(r, \varphi, t) = \sum_{m=1}^{\infty} \left\{C_m I_{m/2\alpha}\left(\sqrt{\frac{s}{v}}r\right) + D_m K_{m/2\alpha}\left(\sqrt{\frac{s}{v}}r\right) - \frac{A_m v}{s} r^{m/2\alpha} - \frac{B_m v}{s} r^{-m/2\alpha}\right\} \sin\left(\frac{m}{2\alpha}\varphi\right) e^{st}. \tag{15}$$

According to equation (10) the velocity distribution is given by

$$u(r, \varphi, t) = \sum_{m=1}^{\infty} \frac{m}{2\alpha}\left\{\frac{A_m v}{s} r^{m/2\alpha - 1} + \frac{B_m v}{s} r^{-m/2\alpha - 1} - \frac{C_m}{r} I_{m/2\alpha}\left(\sqrt{\frac{s}{v}}r\right) - \frac{D_m}{r} K_{m/2\alpha}\left(\sqrt{\frac{s}{v}}r\right)\right\} \cos\left(\frac{m}{2\alpha}\varphi\right) e^{st}, \tag{16a}$$

$$v(r, \varphi, t) = \sum_{m=1}^{\infty} \left\{\frac{m}{2\alpha}\left(-\frac{A_m v}{r} r^{m/2\alpha - 1} + \frac{B_m v}{r} r^{m/2\alpha - 1}\right) + C_m\sqrt{\frac{s}{v}} I'_{m/2\alpha}\left(\sqrt{\frac{s}{v}}r\right) + D_m\sqrt{\frac{s}{v}} K'_{m/2\alpha}\left(\sqrt{\frac{s}{v}}r\right)\right\} \sin\left(\frac{m}{2\alpha}\varphi\right) e^{st}, \tag{16b}$$

where the prime denotes differentiation with respect to r. It is noted that $v = 0$ for $\varphi = 0$ and $2\pi\alpha$.

The solution of equation (12) for the pressure distribution yields

$$p(r, \varphi, t) = \sum_{m=1}^{\infty} [\Gamma_m r^{m/2\alpha} + \Lambda_m r^{-m/2\alpha}] \cos\left(\frac{m}{2\alpha}\varphi\right) e^{st}. \tag{17}$$

Combining the free surface conditions (5) and (6), after differentiation with respect to time, yields the expression

$$\frac{\partial^2 u}{\partial \varphi^2} + u + \frac{a^2}{\sigma}\frac{\partial p}{\partial t} - \frac{2\mu a^2}{\sigma}\frac{\partial^2 u}{\partial r\,\partial t} = 0 \qquad \text{at } r = a. \tag{18}$$

In addition, by introducing the pressure (17) and (16a, b) into the Stokes equation, we obtain the relation between the constants A_m, B_m and Γ_m, Λ_m, namely

$$\Gamma_m = -\mu A_m, \qquad \Lambda_m = \mu B_m. \tag{19}$$

With the boundary condition at the rigid shell wall at $r = b$, i.e.,

$$u = v = 0 \qquad \text{at } r = b, \tag{20}$$

we obtain the equations for $m = 1, 2, \ldots$

$$\bar{A}_m k^{m/2\alpha} + \bar{B}_m k^{-m/2\alpha} - C_m S \mathrm{I}_{m/2\alpha}(k\sqrt{S}) - D_m S \mathrm{K}_{m/2\alpha}(k\sqrt{S}) = 0 \tag{21a}$$

$$-\bar{A}_m \frac{m}{2\alpha} k^{m/2\alpha} + \bar{B}_m \frac{m}{2\alpha} k^{-m/2\alpha} + C_m S\sqrt{S} k \mathrm{I}'_{m/2\alpha}(k\sqrt{S}) + D_m S\sqrt{S} k \mathrm{K}'_{m/2\alpha}(k\sqrt{S}) = 0, \tag{21b}$$

where

$$\frac{sa^2}{v} \equiv S, \quad \frac{b}{a} \equiv k, \quad A_m a^{m/2\alpha+2} \equiv \bar{A}_m, \quad B_m a^{-m/2\alpha+2} \equiv \bar{B}_m.$$

The shear stress at the surface of the liquid, i.e., equation (7), yields

$$-\bar{A}_m \frac{m}{\alpha}\left(\frac{m}{2\alpha} - 1\right) - \bar{B}_m \frac{m}{\alpha}\left(\frac{m}{2\alpha} + 1\right) + C_m S\left[\left(S + \frac{m^2}{2\alpha^2}\right)\mathrm{I}_{m/2\alpha}(\sqrt{S}) - 2\sqrt{S}\,\mathrm{I}'_{m/2\alpha}(\sqrt{S})\right]$$

$$+ D_m S\left[\left(S + \frac{m^2}{2\alpha^2}\right)\mathrm{K}_{m/2\alpha}(\sqrt{S}) - 2\sqrt{S}\,\mathrm{K}'_{m/2\alpha}(\sqrt{S})\right] = 0 \qquad \text{for } m = 1, 2, \ldots \tag{22}$$

Finally, the combined free surface condition (18) results in equation

$$\bar{A}_m\left[\frac{m}{2\alpha}\left(1 - \frac{m^2}{4\alpha^2}\right) - S^2\left(\frac{\rho v^2}{\sigma a}\right) - \frac{m}{\alpha}\left(\frac{m}{2\alpha} - 1\right)S\left(\frac{\rho v^2}{\sigma a}\right)\right]$$

$$+ \bar{B}_m\left[\frac{m}{2\alpha}\left(1 - \frac{m^2}{4\alpha^2}\right) + S^2\left(\frac{\rho v^2}{\sigma a}\right) + \frac{m}{\alpha}\left(\frac{m}{2\alpha} + 1\right)S\left(\frac{\rho v^2}{\sigma a}\right)\right]$$

$$+ C_m S\left[\frac{m}{2\alpha}\left(\frac{m^2}{4\alpha^2}-1\right)\mathrm{I}_{m/2\alpha}(\sqrt{S})+\frac{m}{\alpha}S\left(\frac{\rho v^2}{\sigma a}\right)(\sqrt{S})\mathrm{I}'_{m/2\alpha}(\sqrt{S})-\mathrm{I}_{m/2\alpha}(\sqrt{S})\right]$$

$$+ D_m S\left[\frac{m}{2\alpha}\left(\frac{m^2}{4\alpha^2}-1\right)\mathrm{K}_{m/2\alpha}(\sqrt{S})+\frac{m}{\alpha}S\left(\frac{\rho v^2}{\sigma a}\right)(\sqrt{S})\mathrm{K}'_{m/2\alpha}(\sqrt{S})-\mathrm{K}_{m/2\alpha}(\sqrt{S})\right]=0. \tag{23}$$

The vanishing coefficient determinant of equations (21a, b), (22) and (23) represents the frequency equation, which may be used for the determination of the damped liquid frequencies S. It should be emphasized here again that the adhesion condition at the rigid wall boundaries $\varphi = 0$ and $2\pi\alpha$ has been abandoned and that, in the case treated above involving slipping edges, the contact angle of the liquid surface (contact line) with the wall is $\frac{1}{2}\pi$.

3.2. Uncoupled Shell Motion

Without liquid the right-hand sides of equations (8) and (9) vanish. With

$$\xi(\varphi, t) = X\mathrm{e}^{\lambda\varphi}\mathrm{e}^{\mathrm{i}\omega t}, \qquad \eta(\varphi, t) = Y\mathrm{e}^{\lambda\varphi}\mathrm{e}^{\mathrm{i}\omega t}, \tag{24}$$

the characteristic equation, that has to be solved for the determination of λ, reads

$$\lambda^6 + \lambda^4(2+\chi) + \lambda^2\left[1+\chi\left(2-\frac{12b^2}{h^2}\right)\right] + \chi\left[1+\frac{12b^2}{h^2}(1-\chi)\right] = 0, \tag{25}$$

where

$$\chi \equiv \omega^2\frac{\bar{\rho}(1-\bar{\nu}^2)b^2}{E} > 0.$$

The solution of the bicubic equation (25) yields $\lambda_j(\chi)$, $j = 1, 2, \ldots, 6$. Then, with the boundary conditions of the clamped shell, i.e.,

$$\xi = \eta = \frac{\partial\xi}{\partial\varphi} = 0 \qquad \text{at } \varphi = 0 \text{ and } 2\pi\alpha, \tag{26}$$

one obtains six algebraic equations, the vanishing coefficient determinant of which represents the frequency equation of the elastic shell [see Bauer & Komatsu (1994)].

3.3. Uncoupled Viscous Liquid Oscillations with Anchored Edges

In this case we omit the boundary condition $u = 0$ at $\varphi = 0, 2\pi\alpha$, and we replace it by the weaker condition, the stuck-edge condition of a vanishing liquid surface displacement at the edge, i.e., $\zeta = 0$ at $\varphi = 0, 2\pi\alpha$. This anchored edge condition is satisfied by a sharp-edged rim and a large tension (see Figure 1) of the liquid. It guarantees the vanishing liquid surface displacement $\zeta = 0$ at locations $\varphi = 0$ and $2\pi\alpha$. The adhesion condition is then only satisfied at $r = b$ and a ($u = 0$) and not in the total region $b < r < a$. Since we deal, however, with liquid of very low viscosity ($\nu = 10^{-6}\,\mathrm{m}^2/\mathrm{s}$ for water), the neglected viscosity effect in this region is (because of the very thin boundary layer) not too large. In any case, the radial velocity u at the side walls for this weaker condition of an anchored case is quite reduced as

compared to the case with the slipping assumption, thus yielding an improved approximate solution of the posed hydroelastic problem. The previous solution (16a, b) satisfies the Stokes equation, the continuity equation and the normal velocity boundary condition $v = 0$ at $\varphi = 0,\ 2\pi\alpha$. With the free surface displacement

$$\zeta(\varphi, t) = \mathrm{e}^{st} \sum_{m=1}^{\infty} \zeta_m \cos\left(\frac{m}{2\alpha}\varphi\right), \tag{27}$$

the kinematic condition (5) gives

$$\frac{v}{a}\zeta_m = \frac{m}{2\alpha}\left[\frac{\bar{A}_m}{S^2} + \frac{\bar{B}_m}{S^2} - \frac{C_m}{S}\mathrm{I}_{m/2\alpha}(\sqrt{S}) - \frac{\mathrm{D}_m}{S}\mathrm{K}_{m/2\alpha}(\sqrt{S})\right]. \tag{28}$$

The dynamic condition (6) is then used, with $\zeta(\varphi, t) = \mathrm{e}^{st}\bar{\zeta}(\varphi)$, yielding

$$\begin{aligned}\frac{\mathrm{d}^2\bar{\zeta}}{\mathrm{d}\varphi^2} + \bar{\zeta} = {} & \frac{a}{v}\left(\frac{\rho v^2}{\sigma a}\right)\sum_{m=1}^{\infty}(\bar{A}_m - \bar{B}_m)\cos\left(\frac{m}{2\alpha}\varphi\right) \\ & + 2\left(\frac{\rho v^2}{\sigma a}\right)\frac{a}{v}\sum_{m=1}^{\infty}\left[\frac{m}{2\alpha}\left(\frac{m}{2\alpha}-1\right)\frac{\bar{A}_m}{S} - \frac{m}{2\alpha}\left(\frac{m}{2\alpha}+1\right)\frac{\bar{B}_m}{S}\right. \\ & - \frac{m}{2\alpha}C_m\{\sqrt{S}\mathrm{I}'_{m/2\alpha}(\sqrt{S}) - \mathrm{I}_{m/2\alpha}(\sqrt{S})\} \\ & \left. - \frac{m}{2\alpha}D_m\{\sqrt{S}\mathrm{K}'_{m/2\alpha}(\sqrt{S}) - \mathrm{K}_{m/2\alpha}(\sqrt{S})\}\right]\cos\left(\frac{m}{2\alpha}\varphi\right),\end{aligned} \tag{29}$$

and leads to the solution

$$\begin{aligned}\bar{\zeta}(\varphi) = {} & A\cos\varphi + B\sin\varphi \\ & - \frac{a}{v}\left(\frac{\rho v^2}{\sigma a}\right)\sum_{m=1}^{\infty}\frac{(\bar{A}_m - \bar{B}_m)}{(m^2/4\alpha^2 - 1)}\cos\left(\frac{m}{2\alpha}\varphi\right) - 2\left(\frac{\rho v^2}{\sigma a}\right)\frac{a}{v}\sum_{m=1}^{\infty}\left[\frac{m}{2\alpha}\left(\frac{m}{2\alpha}-1\right)\frac{\bar{A}_m}{S}\right. \\ & - \frac{m}{2\alpha}\left(\frac{m}{2\alpha}+1\right)\frac{\bar{B}_m}{S} - \frac{m}{2\alpha}C_m\{\sqrt{S}\mathrm{I}'_{m/2\alpha}(\sqrt{S}) - \mathrm{I}_{m/2\alpha}(\sqrt{S})\} \\ & \left. - \frac{m}{2\alpha}D_m\{\sqrt{S}\mathrm{K}'_{m/2\alpha}(\sqrt{S}) - \mathrm{K}_{m/2\alpha}(\sqrt{S})\}\right]\frac{1}{(m^2/4\alpha^2 - 1)}\cos\left(\frac{m}{2\alpha}\varphi\right).\end{aligned} \tag{30}$$

The anchored edge condition $\zeta = 0$ at $\varphi = 0,\ 2\pi\alpha$ gives two equations:

$$\begin{aligned}A - {} & \frac{a}{v}\left(\frac{\rho v^2}{\sigma a}\right)\sum_{m=1}^{\infty}\frac{(\bar{A}_m - \bar{B}_m)}{(m^2/4\alpha^2 - 1)} - 2\left(\frac{\rho v^2}{\sigma a}\right)\frac{a}{v}\sum_{m=1}^{\infty}\left[\frac{m}{2\alpha}\left(\frac{m}{2\alpha}-1\right)\frac{\bar{A}_m}{S}\right. \\ & - \frac{m}{2\alpha}\left(\frac{m}{2\alpha}+1\right)\frac{\bar{B}_m}{S} - \frac{m}{2\alpha}C_m[\sqrt{S}\mathrm{I}'_{m/2\alpha}(\sqrt{S}) - \mathrm{I}_{m/2\alpha}(\sqrt{S})] \\ & \left. - \frac{m}{2\alpha}D_m\{\sqrt{S}\mathrm{K}'_{m/2\alpha}(\sqrt{S}) - \mathrm{K}_{m/2\alpha}(\sqrt{S})\}\right]\frac{1}{(m^2/4\alpha^2 - 1)} = 0\end{aligned} \tag{31a}$$

and

$$A\cos(2\pi\alpha) + B\sin(2\pi\alpha) - \frac{a}{v}\left(\frac{\rho v^2}{\sigma a}\right)\sum_{m=1}^{\infty}(-1)^m\frac{(\bar{A}_m - \bar{B}_m)}{(m^2/4\alpha^2 - 1)}$$
$$- 2\left(\frac{\rho v^2}{\sigma a}\right)\frac{a}{v}\sum_{m=1}^{\infty}\left[\frac{m}{2\alpha}\left(\frac{m}{2\alpha} - 1\right)\frac{\bar{A}_m}{S} - \frac{m}{2\alpha}\left(\frac{m}{2\alpha} + 1\right)\frac{\bar{B}_m}{S}\right.$$
$$- \frac{m}{2\alpha}C_m\{\sqrt{S}\,\mathrm{I}'_{m/2\alpha}(\sqrt{S}) - \mathrm{I}_{m/2\alpha}(\sqrt{S})\}$$
$$\left. - \frac{m}{2\alpha}D_m\{\sqrt{S}\,\mathrm{K}'_{m/2\alpha}(\sqrt{S}) - \mathrm{K}_{m/2\alpha}(\sqrt{S})\}\right]\frac{(-1)^m}{(m^2/4\alpha^2 - 1)} = 0. \tag{31b}$$

Utilizing the expansions

$$\cos\varphi = \frac{\sin 2\pi\alpha}{2\pi\alpha} + \sum_{m=1}^{\infty}\frac{(-1)^{m-1}\sin 2\pi\alpha}{\pi\alpha(m^2/4\alpha^2 - 1)}\cos\left(\frac{m}{2\alpha}\varphi\right)$$

and

$$\sin\varphi = \frac{1 - \cos 2\pi\alpha}{2\pi\alpha} + \sum_{m=1}^{\infty}\frac{[(-1)^m\cos 2\pi\alpha - 1]}{\pi\alpha(m^2/4\alpha^2 - 1)}\cos\left(\frac{m}{2\alpha}\varphi\right)$$

and introducing them into equation (30), equating it to (27), and comparing coefficients, the following equation is obtained:

$$\frac{\bar{A}(-1)^{m-1}\sin 2\pi\alpha}{\pi\alpha} + \frac{\bar{B}\{(-1)^m\cos 2\pi\alpha - 1\}}{\pi\alpha}$$
$$+ \bar{A}_m\left[\left(\frac{\rho v^2}{\sigma a}\right)\left\{-1 - \frac{(m/\alpha)(m/2\alpha - 1)}{S}\right\} - \frac{m}{2\alpha}\frac{(m^2/4\alpha^2 - 1)}{S^2}\right]$$
$$+ \bar{B}_m\left[\left(\frac{\rho v^2}{\sigma a}\right)\left\{1 + \frac{(m/\alpha)(m/2\alpha + 1)}{S}\right\} - \frac{m}{2\alpha}\frac{(m^2/4\alpha^2 - 1)}{S^2}\right]$$
$$+ C_m\frac{m}{2\alpha}\left[2\left(\frac{\rho v^2}{\sigma a}\right)\{\sqrt{S}\,\mathrm{I}'_{m/2\alpha}(\sqrt{S}) - \mathrm{I}_{m/2\alpha}(\sqrt{S})\} + \frac{(m^2/4\alpha^2 - 1)}{S}\mathrm{I}_{m/2\alpha}(\sqrt{S})\right]$$
$$+ D_m\frac{m}{2\alpha}\left[2\left(\frac{\rho v^2}{\sigma a}\right)\{\sqrt{S}\,\mathrm{K}'_{m/2\alpha}(\sqrt{S}) - \mathrm{K}_{m/2\alpha}(\sqrt{S})\}\right.$$
$$\left. + \frac{(m^2/4\alpha^2 - 1)}{S}\mathrm{K}_{m/2\alpha}(\sqrt{S})\right] = 0 \qquad \text{for } m = 1, 2, \ldots, \tag{32}$$

where

$$\bar{A} \equiv \frac{v}{a}A, \qquad \bar{B} \equiv \frac{v}{a}B.$$

With the shear stress condition (22), equations (31a, b), (32) and (21a, b) we have a total of $(4m + 2)$ equations in $\bar{A}$, $\bar{B}$, $\bar{A}_m$, $\bar{B}_m$, C_m and D_m. The vanishing coefficient determinant

represents the frequency equation for the anchored-edge liquid case. Truncating this infinite determinant to one of finite order gives the approximate value of the lower frequencies. It should be noticed that the constants of equation (28) have been determined to satisfy the anchored edge conditions $\zeta = 0$ at $\varphi = 2\pi\alpha$ [see equation (32)].

3.4. Coupled Hydroelastic Solution with Freely Slipping Edges

In the coupled hydroelastic case, equations (8) and (9) with the right-hand side included i.e., with the influence of the viscous liquid taken into account, have to be solved. Substituting equations (16) and (17) into these equations yields

$$\frac{\partial^4\xi}{\partial\varphi^4} + 2\frac{\partial^2\xi}{\partial\varphi^2} + \left(1 + \frac{12b^2}{h^2}\right)\xi + \frac{12b^2}{h^2}\frac{\partial\eta}{\partial\varphi} + \frac{12\bar{\rho}(1-\bar{\nu}^2)b^4}{Eh^2}\frac{\partial^2\xi}{\partial t^2} = \frac{b}{v}\sum_{m=1}^{\infty} E_m \cos\left(\frac{m}{2\alpha}\varphi\right)\mathrm{e}^{st} \tag{33a}$$

and

$$\frac{\partial\xi}{\partial\varphi} + \frac{\partial^2\eta}{\partial\varphi^2} - \frac{\bar{\rho}(1-\bar{\nu}^2)b^2}{E}\frac{\partial^2\eta}{\partial t^2} = \frac{b}{v}\sum_{m=1}^{\infty} F_m \sin\left(\frac{m}{2\alpha}\varphi\right)\mathrm{e}^{st}, \tag{33b}$$

where

$$E_m = e_a\bar{A}_m + e_b\bar{B}_m + e_cC_m + e_dD_m, \tag{34a}$$

$$e_a = P\left[k^2 + \frac{m}{\alpha}\frac{1}{k^2S}\left(\frac{m}{2\alpha} - 1\right)\right]k^{m/2\alpha},$$

$$e_b = P\left[-k^2 - \frac{m}{\alpha}\frac{1}{k^2S}\left(\frac{m}{2\alpha} + 1\right)\right]k^{-m/2\alpha},$$

$$e_c = \frac{m}{\alpha}P\left[\mathrm{I}_{m/2\alpha}(k\sqrt{S}) - k\sqrt{S}\,\mathrm{I}'_{m/2\alpha}(k\sqrt{S})\right],$$

$$e_d = \frac{m}{\alpha}P\left[\mathrm{K}_{m/2\alpha}(k\sqrt{S}) - k\sqrt{S}\,\mathrm{K}'_{m/2\alpha}(k\sqrt{S})\right],$$

$$F_m = f_a\bar{A}_m + f_b\bar{B}_m + f_cC_m + f_dD_m, \tag{34b}$$

$$f_a = Q\frac{m}{2\alpha}\frac{1}{S}\left(2 - \frac{m}{\alpha}\right)k^{m/2\alpha}, \quad f_b = Q\frac{m}{2\alpha}\frac{1}{S}\left(-2 - \frac{m}{\alpha}\right)k^{-m/2\alpha},$$

$$f_c = Q\left[-k\sqrt{S}\,\mathrm{I}'_{m/2\alpha}(k\sqrt{S}) + k^2S\,\mathrm{I}''_{m/2\alpha}(k\sqrt{S}) + \left(\frac{m}{2\alpha}\right)^2\mathrm{I}_{m/2\alpha}(k\sqrt{S})\right],$$

$$f_d = Q\left[-k\sqrt{S}\,\mathrm{K}'_{m/2\alpha}(k\sqrt{S}) + k^2S\,\mathrm{K}''_{m/2\alpha}(k\sqrt{S}) + \left(\frac{m}{2\alpha}\right)^2\mathrm{K}_{m/2\alpha}(k\sqrt{S})\right],$$

$$P \equiv 12\gamma\frac{\rho}{\bar{\rho}}\left(\frac{b}{h}\right)^3, \qquad Q \equiv \gamma\frac{b}{h}\frac{\rho}{\bar{\rho}}, \qquad \gamma \equiv \frac{\bar{\rho}(1-\bar{\nu}^2)v^2}{Eb^2}.$$

The solution is given by

$$\xi(\varphi, t) = e^{st}\left[\sum_{j=1}^{6} X_j e^{\lambda_j \varphi} + \frac{b}{v}\sum_{m=1}^{\infty} \hat{E}_m \cos\left(\frac{m}{2\alpha}\varphi\right)\right], \tag{35a}$$

$$\eta(\varphi, t) = e^{st}\left[\sum_{j=1}^{6} \frac{-\lambda_j}{\lambda_j^2 + \hat{\chi}} X_j e^{\lambda_j \varphi} + \frac{b}{v}\sum_{m=1}^{\infty} \hat{F}_m \sin\left(\frac{m}{2\alpha}\varphi\right)\right], \tag{35b}$$

where $\hat{\chi}$, $\hat{E}_m$ and $\hat{F}_m$ are

$$\hat{\chi} = -\frac{\bar{\rho}(1-\bar{\nu}^2)b^2 s^2}{E},$$

$$\hat{E}_m = \frac{1}{\Delta_m}\left[\left\{\hat{\chi} - \left(\frac{m}{2\alpha}\right)^2\right\} E_m - \frac{12b^2}{h^2} F_m\right],$$

$$\hat{F}_m = \frac{1}{\Delta_m}\left[\left\{\left(\frac{m}{2\alpha}\right)^4 - 2\left(\frac{m}{2\alpha}\right)^2 + 1 + \frac{12b^2}{h^2}(1-\hat{\chi})\right\} F_m + \frac{m}{2\alpha} E_m\right],$$

$$\Delta_m = \left\{\left(\frac{m}{2\alpha}\right)^4 - 2\left(\frac{m}{2\alpha}\right)^2 + 1 + \frac{12b^2}{h^2}(1-\hat{\chi})\right\}\left\{\hat{\chi} - \left(\frac{m}{2\alpha}\right)^2\right\} + \left(\frac{m}{2\alpha}\right)^2 \frac{12b^2}{h^2},$$

and X_j are determined by the shell boundary condition

$$\xi = \eta = \frac{\partial \xi}{\xi \varphi} = 0, \qquad \text{at } \varphi = 0, 2\pi\alpha.$$

Then six algebraic equations are derived as follows:

$$\sum_{j=1}^{6} X_j = -\sum_{m=1}^{\infty} \frac{b}{v}\hat{E}_m, \qquad \sum_{j=1}^{6} \frac{-\lambda_j}{\lambda_j^2 + \hat{\chi}} X_j = 0,$$

$$\sum_{j=1}^{6} \lambda_j X_j = 0, \qquad \sum_{j=1}^{6} X_j e^{2\pi\alpha\lambda_j} = -\sum_{m=1}^{\infty} \frac{b}{v}\hat{E}_m (-1)^m,$$

$$\sum_{j=1}^{6} \frac{-\lambda_j}{\lambda_j^2 + \hat{\chi}} X_j e^{2\pi\alpha\lambda_j} = 0, \qquad \sum_{j=1}^{6} \lambda_j X_j e^{2\pi\alpha\lambda_j} = 0.$$

Solving these equations simultaneously, the X_j is obtained as a linear combination of $\hat{E}_m$,

$$X_j = \frac{b}{v} H_j \sum_{m=1}^{\infty} \hat{E}_m. \tag{36}$$

Introducing ξ and η from equations (35) and u and v from equations (16), the compatibility conditions at the shell

$$\frac{\partial \xi}{\partial t} = u, \qquad \frac{\partial \eta}{\partial t} = v \qquad \text{at } r = b$$

give

$$\sum_{m=1}^{\infty}\left\{\left[k^2 S^2\left\{\sum_{j=1}^{6} H_j e^{\lambda_j \varphi} + \cos\left(\frac{m}{2\alpha}\varphi\right)\right\} e_m^a - \frac{m}{2\alpha} r^{m/2\alpha} \cos\left(\frac{m}{2\alpha}\varphi\right)\right] \bar{A}_m\right.$$

$$\left. + \left[k^2 S^2\left\{\sum_{j=1}^{6} H_j e^{\lambda_j \varphi} + \cos\left(\frac{m}{2\alpha}\varphi\right)\right\} e_m^b - \frac{m}{2\alpha} k^{-m/2\alpha} \cos\left(\frac{m}{2\alpha}\varphi\right)\right] \bar{B}_m\right.$$

$$+\left[k^2S^2\left\{\sum_{j=1}^{6}H_j e^{\lambda_j\varphi}+\cos\left(\frac{m}{2\alpha}\varphi\right)\right\}e_m^c+\frac{m}{2\alpha}S\mathrm{I}_{m/2\alpha}(k\sqrt{S})\cos\left(\frac{m}{2\alpha}\varphi\right)\right]C_m$$

$$+\left[k^2S^2\left\{\sum_{j=1}^{6}H_j e^{\lambda_j\varphi}+\cos\left(\frac{m}{2\alpha}\varphi\right)\right\}e_m^d+\frac{m}{2\alpha}S\mathrm{K}_{m/2\alpha}(k\sqrt{S})\cos\left(\frac{m}{2\alpha}\varphi\right)\right]D_m\Bigg\}=0, \quad (37a)$$

$$\sum_{m=1}^{\infty}\Bigg\{\left[k^2S^2\left\{\sum_{j=1}^{6}\frac{-\lambda_jH_j}{\lambda_j^2+\hat{\chi}}e^{\lambda_j\varphi}e_m^a+f_m^a\sin\left(\frac{m}{2\alpha}\varphi\right)\right\}+\frac{m}{2\alpha}k^{m/2\alpha}\sin\left(\frac{m}{2\alpha}\varphi\right)\right]\bar{A}_m$$

$$+\left[k^2S^2\left\{\sum_{j=1}^{6}\frac{-\lambda_jH_j}{\lambda_j^2+\hat{\chi}}e^{\lambda_j\varphi}e_m^b+f_m^b\sin\left(\frac{m}{2\alpha}\varphi\right)\right\}-\frac{m}{2\alpha}k^{-m/2\alpha}\sin\left(\frac{m}{2\alpha}\varphi\right)\right]\bar{B}_m$$

$$+\left[k^2S^2\left\{\sum_{j=1}^{6}\frac{-\lambda_jH_j}{\lambda_j^2+\hat{\chi}}e^{\lambda_j\varphi}e_m^c+f_m^c\sin\left(\frac{m}{2\alpha}\varphi\right)\right\}-S\sqrt{S}k\mathrm{I}'_{m/2\alpha}(k\sqrt{S})\sin\left(\frac{m}{2\alpha}\varphi\right)\right]C_m$$

$$+\left[k^2S^2\left\{\sum_{j=1}^{6}\frac{-\lambda_jH_j}{\lambda_j^2+\hat{\chi}}e^{\lambda_j\varphi}e_m^d+f_m^d\sin\left(\frac{m}{2\alpha}\varphi\right)\right\}\right.$$

$$\left.-S\sqrt{S}k\mathrm{K}'_{m/2\alpha}(k\sqrt{S})\sin\left(\frac{m}{2\alpha}\varphi\right)\right]D_m\Bigg\}=0 \quad (37b)$$

where

$$e_m^a=\frac{1}{\Delta_m}\left[\left\{\hat{\chi}-\left(\frac{m}{2\alpha}\varphi\right)^2\right\}e_a-\frac{12b^2}{h^2}\frac{m}{2\alpha}f_a\right],$$

$$f_m^a=\frac{1}{\Delta_m}\left[\left\{\left(\frac{m}{2\alpha}\varphi\right)^4-2\left(\frac{m}{2\alpha}\varphi\right)^2+1+\frac{12b^2}{h^2}(1-\hat{\chi})\right\}f_a+\frac{m}{2\alpha}e_a\right];$$

e_m^b, e_m^c, e_m^d, f_m^b, f_m^c and f_m^d are almost the same expressions except for the superscripts a, b, c and d.

Then, $e^{\lambda_j\varphi}$ is expanded into Fourier-cosine series for equation (37a) and Fourier-sine series for equation (37b) in the region $0\leqslant\varphi\leqslant 2\pi\alpha$ as

$$e^{\lambda_j\varphi}=\frac{e^{2\pi\alpha\lambda_j}-1}{2\pi\alpha\lambda_j}+\sum_{m=1}^{\infty}\frac{4\alpha\lambda_j\{e^{2\pi\alpha\lambda_j}(-1)^m-1\}}{\pi\{m^2+(2\alpha\lambda_j)^2\}}\cos\left(\frac{m}{2\alpha}\varphi\right),$$

$$e^{\lambda_j\varphi}=\sum_{m=1}^{\infty}\frac{2m\{1-e^{2\pi\alpha\lambda_j}(-1)^m\}}{\pi\{m^2+(2\alpha\lambda_j)^2\}}\sin\left(\frac{m}{2\alpha}\varphi\right).$$

By comparing coefficients of $\cos[(m/2\alpha)\varphi]$ and $\sin[(m/2\alpha)\varphi]$ yields

$$\left[k^2S^2\left\{\sum_{j=1}^{6}H_j\frac{4\alpha\lambda_j[e^{2\pi\alpha\lambda_j}(-1)^m-1]}{\pi[m^2+(2\alpha\lambda_j)^2]}+1\right\}e_m^a-\frac{m}{2\alpha}k^{m/2\alpha}\right]\bar{A}_m$$

$$+\left[k^2S^2\left\{\sum_{j=1}^{6}H_j\frac{4\alpha\lambda_j[e^{2\pi\alpha\lambda_j}(-1)^m-1]}{\pi[m^2+(2\alpha\lambda_j)^2]}+1\right\}e_m^b-\frac{m}{2\alpha}k^{-m/2\alpha}\right]\bar{B}_m$$

$$+\left[k^2S^2\left\{\sum_{j=1}^{6} H_j\frac{4\alpha\lambda_j[\mathrm{e}^{2\pi\alpha\lambda_j}(-1)^m-1]}{\pi[m^2+(2\alpha\lambda_j)^2]}+1\right\}e_m^c+\frac{m}{2\alpha}S\mathrm{I}_{m/2\alpha}(k\sqrt{S})\right]C_m$$

$$+\left[k^2S^2\left\{\sum_{j=1}^{6} H_j\frac{4\alpha\lambda_j[\mathrm{e}^{2\pi\alpha\lambda_j}(-1)^m-1]}{\pi[m^2+(2\alpha\lambda_j)^2]}+1\right\}e_m^d+\frac{m}{2\alpha}S\mathrm{K}_{m/2\alpha}(k\sqrt{S})\right]D_m=0, \tag{38a}$$

$$\left[k^2S^2\left\{\sum_{j=1}^{6}\frac{-\lambda_jH_j}{\lambda_j^2+\hat{\chi}}\frac{2m[1-\mathrm{e}^{2\pi\alpha\lambda_j}(-1)^m]}{\pi[m^2+(2\alpha\lambda_j)^2]}e_m^a+f_m^a\right\}+\frac{m}{2\alpha}k^{m/2\alpha}\right)\right]\bar{A}_m$$

$$+\left[k^2S^2\left\{\sum_{j=1}^{6}\frac{-\lambda_jH_j}{\lambda_j^2+\hat{\chi}}\frac{2m[1-\mathrm{e}^{2\pi\alpha\lambda_j}(-1)^m]}{\pi[m^2+(2\alpha\lambda_j)^2]}e_m^b+f_m^b\right\}-\frac{m}{2\alpha}k^{-m/2\alpha}\right)\right]\bar{B}_m$$

$$+\left[k^2S^2\left\{\sum_{j=1}^{6}\frac{-\lambda_jH_j}{\lambda_j^2+\hat{\chi}}\frac{2m[1-\mathrm{e}^{2\pi\alpha\lambda_j}(-1)^m]}{\pi[m^2+(2\alpha\lambda_j)^2]}e_m^c+f_m^c\right\}-S\sqrt{S}k\mathrm{I}'_{m/2\alpha}(k\sqrt{S})\right]C_m$$

$$+\left[k^2S^2\left\{\sum_{j=1}^{6}\frac{-\lambda_jH_j}{\lambda_j^2+\hat{\chi}}\frac{2m[1-\mathrm{e}^{2\pi\alpha\lambda_j}(-1)^m]}{\pi[m^2+(2\alpha\lambda_j)^2]}e_m^d+f_m^d\right\}-S\sqrt{S}k\mathrm{K}'_{m/2\alpha}(k\sqrt{S})\right]D_m=0. \tag{38b}$$

When the shell is rigid, where the coefficients $e_m^a, f_m^a, e_m^b, f_m^b, e_m^c, f_m^c, e_m^d$ and f_m^d become zero, equations (38a, b) coincide with (21a, b). The vanishing coefficient matrix of the $4m$ homogeneous equations (22), (23) and (38a, b) for $\bar{A}_m$, $\bar{B}_m$, C_m and D_m yields the coupled frequencies.

3.5. Coupled Hydroelastic Solution with Anchored Edges

In the case of anchored edges, the solution procedure is almost the same with that of a freely slipping case. The equations (22), (31a, b), (32) and, instead of (21a, b) for a rigid shell, (38a, b) are employed for this case.

4. LIQUID INSIDE AN ELASTIC SHELL

If we want to treat the system consisting of an elastic shell at $r = b$ and an inside liquid with a free surface at $r = a$ ($a/b \leqslant 1$), we have to introduce a minus sign on the right-hand side of equation (5). Accordingly, the equations corresponding to equation (5) must have a minus sign on the appropriate terms. The process for determining the natural and coupled frequencies is similar to that used in the liquid outside case.

5. NUMERICAL EVALUATION AND DISCUSSION

Some of the analytically obtained results have been evaluated numerically for various parameters, i.e., the diameter ratio $k = b/a$, the flexibility parameter $\bar{\rho}(1-\bar{\nu}^2)b^2/E$, the Ohnesorge number $\mathrm{Oh} \equiv \sqrt{\rho\nu^2/\sigma a}$; where the apex angle $2\pi\alpha = \frac{1}{2}\pi$, shell thickness ratio $h/a = 0{\cdot}01$ and density ratio $\bar{\rho}/\rho = 2$ were taken. It was found previously (Bauer & Komatsu 1994) that the undamped natural frequencies decrease with increasing diameter ratio $k = b/a$, i.e., for decreasing liquid layer thickness. In addition, for higher mode

frequencies this decrease is appreciable only for thinner liquid layers. It also was found that the natural liquid frequencies for liquid layers with anchored contact lines are larger than those for freely slipping edges.

In Figures 2 and 3 we represent the coupled oscillation frequencies of the viscous liquid and structure as a function of the flexibility of the shell and compare it with the inviscid liquid case. It may be noticed that for freely slipping edges, the fundamental damped natural sloshing frequency is decreased by the presence of viscosity. In addition, a slight decrease of the oscillation frequency is visible with the increase in flexibility of the structure. This shows that with an increase in the magnitude of $\bar{\rho}(1-\bar{\nu}^2)b^2/E$ (or the decrease in Young's modulus E) the coupled sloshing oscillation frequency is slightly reduced, as has been found previously for inviscid liquid (Bauer & Komatsu 1994). The coupled structural frequency, as

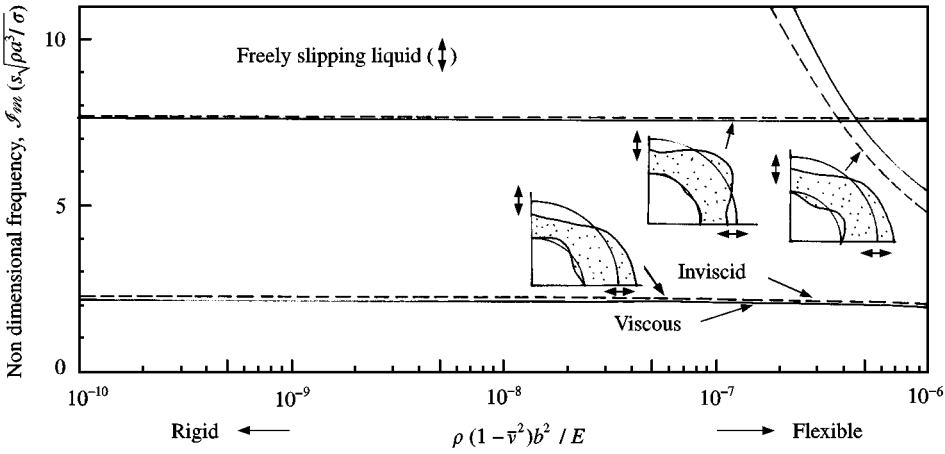

Figure 2. Effect of shell flexibility on the coupled frequencies with freely slipping edges: $b/a = 0.5$, $\rho\nu^2/\sigma a = 10^{-5}$, $\alpha = 0.25$, $\sigma/\rho a^3 = 100$, $h/a = 0.01$, $\bar{\rho}/\rho = 2$.

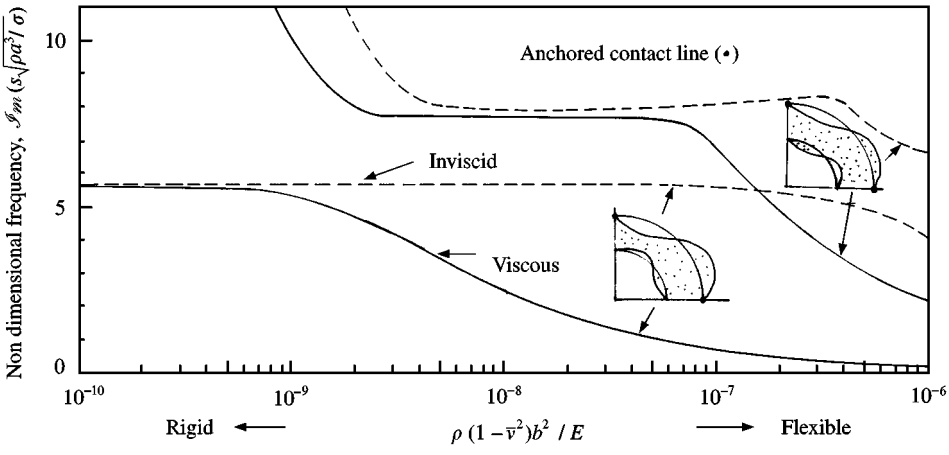

Figure 3. Effect of shell flexibility on the coupled frequencies with anchored edges: $b/a = 0.5$, $\rho\nu^2/\sigma a = 10^{-5}$, $\alpha = 0.25$, $\sigma/\rho a^3 = 100$, $h/a = 0.01$, $\bar{\rho}/\rho = 2$.

shown in the right-hand curve of Figure 2, illustrates that viscosity results in a higher coupled frequency; on the other hand, the coupled frequency is drastically reduced with increasing flexibility of the structure.

For the case of anchored contact lines, the coupled oscillation frequencies are presented in Figure 3. We notice that, in comparison with the inviscid liquid case, the coupled fundamental sloshing frequency for viscous liquid is decreased considerably with increasing flexibility of the structure. The coupled shell frequency shows a similar effect and is smaller in the viscous case than for inviscid liquid.

In Figure 4, the real (– – –) and imaginary (——) parts of the fundamental coupled sloshing frequency are presented as a function of the diameter ratio $k = b/a$, with $\rho v^2/\sigma a$ as a parameter. First of all we notice that the increase in the damping decay (real part) and decrease of the oscillation frequency (imaginary part) as the thickness of the liquid layer is decreased, i.e., $k = b/a$ is increased. The influence of the Ohnesorge number Oh is also presented. The increase of the Ohnesorge number increases the decay magnitude and decreases the oscillation frequency.

In Figure 5 the results for the fundamental sloshing frequency are shown for anchored contact lines. The physical trends are the same, except for larger magnitudes in comparison with the freely slipping case. In addition, we notice a region where only aperiodic motion is possible, for large aspect ratio $k = b/a$.

In Figure 6 the real and imaginary parts of the fundamental sloshing root $s\sqrt{\sigma/\rho a^3}$ for freely slipping contact lines are presented as a function of the Ohnesorge number $(\mathrm{Oh})^2 \equiv \rho v^2/\sigma a$. Two cases are presented: for uncoupled liquid motion, and for the hydroelastic case with an elastic wall at $r = b$. First of all we notice that, with increasing Ohnesorge number Oh, the decay magnitude increases, while the oscillation frequency decreases, reaching finally a vanishing magnitude which indicates that both roots become of

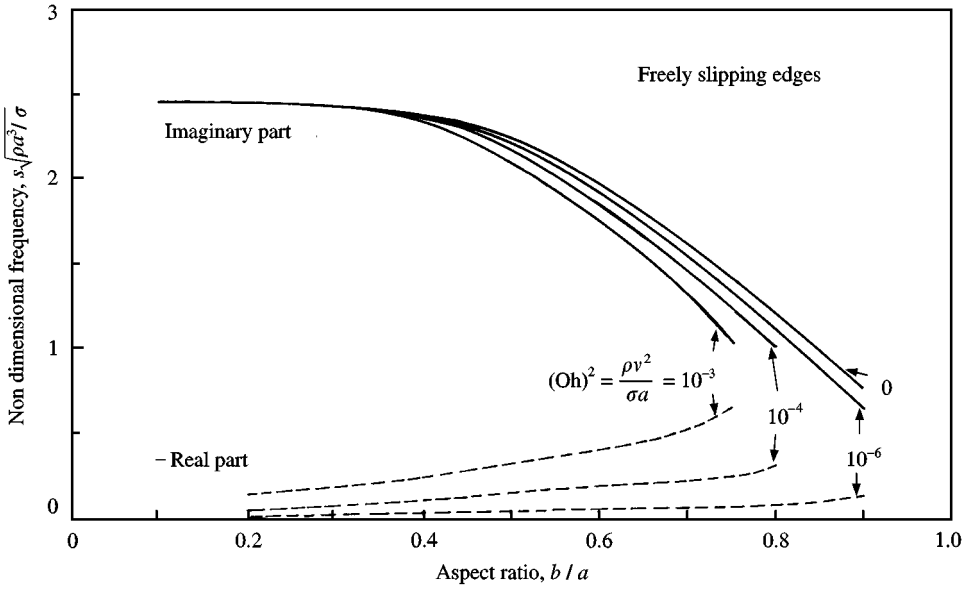

Figure 4. Effect of viscosity (Ohnesorge number) and layer thickness on the fundamental coupled frequency with freely slipping edges: $\bar{\rho}(1-\bar{\nu}^2)b^2/E = 10^{-6}$, $\alpha = 0.25$, $\sigma/\rho a^3 = 100$, $h/a = 0.01$, $\bar{\rho}/\rho = 2$.

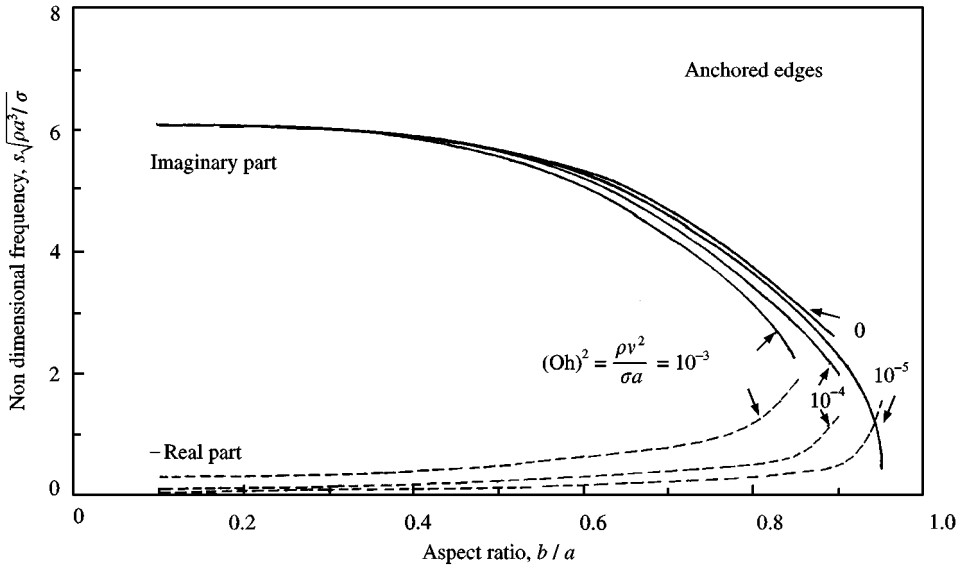

Figure 5. Effect of viscosity (Ohnesorge number) and layer thickness on the fundamental coupled frequency with anchored edges: $\bar{\rho}(1-\bar{\nu}^2)b^2/E = 10^{-6}$, $\alpha = 0.25$, $\sigma/\rho a^3 = 100$, $h/a = 0.01$, $\bar{\rho}/\rho = 2$.

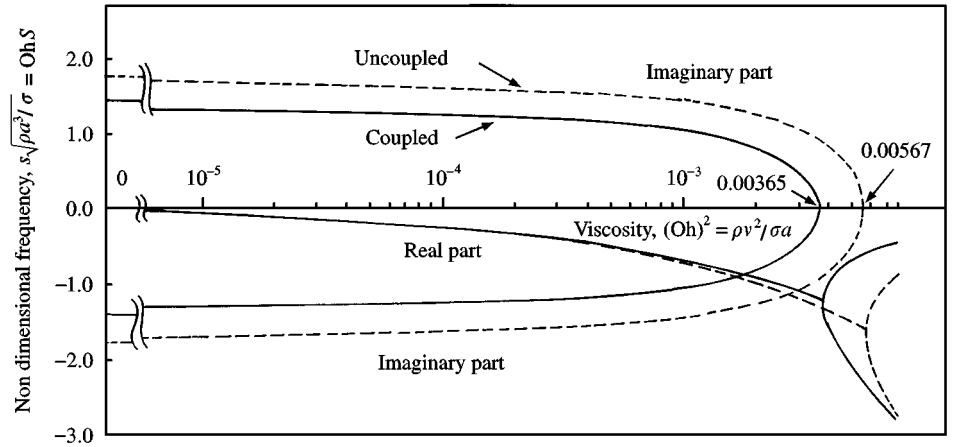

Figure 6. Complex frequency and influence of viscosity of the fundamental coupled and uncoupled vibration mode with freely slipping edges: $\bar{\rho}(1-\bar{\nu}^2)b^2/E = 10^{-6}$, $b/a = 0.75$, $\alpha = 0.25$, $\sigma/\rho a^3 = 100$, $h/a = 0.01$, $\bar{\rho}/\rho = 2$.

negative real magnitude. Therefore, only aperiodic motion is possible in this range. The inclusion of elasticity yields a slightly reduced decay magnitude and a moderately decreased oscillation frequency in comparison with the uncoupled liquid case. The region of only aperiodic motion starts at a small Ohnesorge number, indicating that elasticity enhances the aperiodic motion. This fact is expressed in a more lucid form in the motion-identification graph of Figure 7, where the fundamental sloshing behaviour is shown for the freely slipping edge case as a function of the diameter ratio $k = b/a$. We notice here that for large Ohnesorge numbers, the aperiodic motion appears over a large range of liquid layer

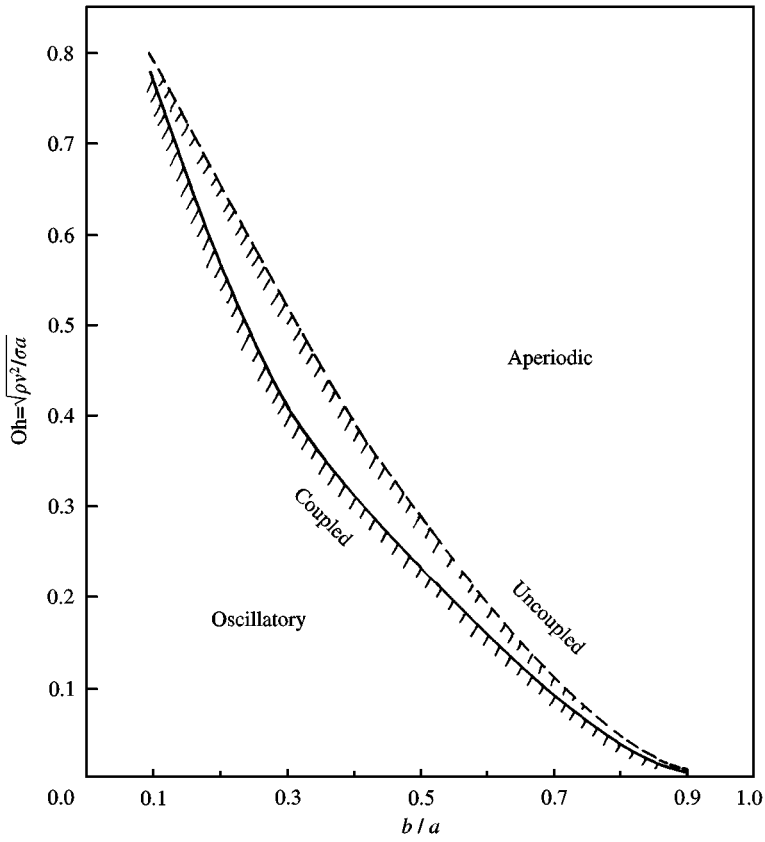

Figure 7. Motion-identification graph for the fundamental vibration mode with freely slipping edges: $\bar{\rho}(1-\bar{\nu}^2)b^2/E = 10^{-6}$, $\alpha = 0.25$, $\sigma/\rho a^3 = 100$, $h/a = 0.01$, $\bar{\rho}/\rho = 2$.

thickness, while small Ohnesorge numbers are associated with decaying oscillatory liquid behaviour. Again, we see that the uncoupled liquid boundary is above that for the case with the elastic circular wall.

In addition, we notice an increase in the aperiodic region with increasing flexibility. The increase of the shell flexibility may be interpreted as a decrease of the stiffness of a spring k. The damping ratio $\zeta = c/2\sqrt{mk}$ (c being the damping and m the mass) therefore increases, thus yielding an enlarged region in which only aperiodic motion is possible. A further increase of the flexibility $\bar{\rho}(1-\bar{\nu}^2)b^2/E$ would produce another curve for the coupled motion in Figure 7, located below the one indicated, thus increasing the region of aperiodic motion even further.

6. CONCLUSIONS

The most important conclusions of the above study may be summarized as follows.

(i) The natural damped frequencies of the sloshing liquid are higher for anchored contact lines than for freely slipping edges.

(ii) The damped liquid oscillation frequencies are smaller than the natural frequencies of the inviscid liquid case.

(iii) With increasing flexibility of the shell, the oscillation frequencies decrease; they are smaller for viscous liquid case than for invisicid liquid case.

(iv) Increasing $k = b/a$, i.e., decreasing the liquid layer thickness, raises the decay magnitude and diminishes the oscillation frequencies; these frequencies are higher for the anchored contact lines case than for the freely slipping case.

(v) Increasing the Ohnesorge number $\mathrm{Oh} \equiv \sqrt{\rho v^2/\sigma a}$ results in a stronger decay magnitude and a higher decrease of oscillation frequencies.

(vi) For large Ohnesorge numbers, the system exhibits a larger range of liquid thicknesses where only aperiodic motion is possible. For small Oh, only a thin layer is able to perform aperiodic motion; while in most of the k-range, oscillatory motion can take place.

(vii) The uncoupled natural frequencies of the shell decrease considerably with increasing shell radius b (Bauer & Komatsu 1994).

(viii) The liquid produces a strong decrease on the coupled shell oscillation frequencies, which is mainly due to the effect of the added liquid mass.

(ix) For thin liquid layers the effect of the sloshing interaction on the elastic frequency is more pronounced.

(x) The interaction effects are more pronounced for liquid with anchored contact lines, since the natural frequency of the liquid is larger than that for freely slipping edges and therefore closer to that of the shell.

References

Abramson, N. H. (ed.) 1966 The dynamic behaviour of liquids in moving containers. NASA SP-106.

Bauer, H. F. 1982 Coupled oscillations of a solidly rotating and non-rotating finite and infinite liquid bridge of immiscible liquids in zero-gravity. *Acta Astronautica* **9,** 547–563.

Bauer, H. F. 1986 Free surface- and interface oscillation of an infinitely long viscoelastic liquid column. *Acta Astronautica* **13,** 9–22.

Bauer, H. F. 1987*a* Natural frequencies and stability of immiscible cylindrical z-independent liquid system. *Applied Microgravity Technology* **1,** 11–26.

Bauer, H. F. 1987*b* Coupled frequencies of a hydroelastic system consisting of an elastic shell and frictionless liquid. *Journal of Sound and Vibration* **113,** 217–232.

Bauer, H. F. 1987*c* Hydroelastic oscillations of a viscous infinitely long liquid column. *Journal of Sound and Vibration* **119,** 249–265.

Bauer, H. F. 1989 Natural frequencies and stability of circular cylindrical immiscible liquid systems. *Applied Microgravity Technology* **2,** 27–44.

Bauer, H. F. & Komatsu, K. 1994 Coupled frequencies of a hydroelastic system of an elastic two-dimensional sector-shell and frictionless liquid in zero-gravity. *Journal of Fluids and Structures* **8,** 817–831.

Lakis, A. A. & Païdoussis, M. P. 1971 Free vibration of cylindrical shells partially filled with liquid. *Journal of Sound and Vibration* **19,** 1–15.

Leissa, A. W. 1973 Vibration of shells. NASA SP-288.

Rayleigh, Lord 1882 On the instability of cylindrical fluid surfaces. *Philosophical Magazine* **34,** 277–283.

Yamaki, N. T., Tani, J. & Yamaji, T. 1984 Free vibration of a clamped-clamped circular cylindrical shell partially filled with liquid. *Journal of Sound and Vibration* **94,** 531–550.

APPENDIX: NOMENCLATURE

a	radius of the equilibrium position of the free liquid surface
b	radius of the shell

$\bar{D}$	$[= Eh/(1-\bar{\nu}^2)]$
E	Young's modulus of elasticity
h	shell thickness
$I_{m/2\alpha}$, $K_{m/2\alpha}$	modified Bessel functions of first and second kind (of order $m/2\alpha$)
k	$(= b/a)$ ratio of radii
Oh	Ohnesorge number $(\equiv \sqrt{\rho\nu^2/\sigma a})$
p	liquid pressure
r, φ	polar coordinates
s	complex frequency $(S \equiv sa^2/\nu)$, $s = \bar{\sigma} \pm i\bar{\omega}$
t	time
u, v	velocity components of the liquid in the radial and circumferential direction, respectively
$2\pi\alpha$	apex angle of sector system
ζ	radial free surface displacement
μ	dynamic viscosity
ν	kinematic viscosity
$\bar{\nu}$	Poisson ratio
ξ, η	radial and circumferential shell deflection, respectively
ρ	density of liquid
$\bar{\rho}$	density of shell
$\bar{\rho}(1-\bar{\nu}^2)/E$	flexibility parameter
σ	liquid surface tension
$\tau_{r\varphi}$	shear stress
Ψ	stream function